Separation of long linear polymers in gel electrophoresis with alternating electric fields: A theoretical study using the necklace model

G. R. Terranova,[1] H. O. Mártin,[1] and C. M. Aldao[2,*]

[1]*Instituto de Investigaciones Físicas de Mar del Plata (IFIMAR), Departamento de Física, Facultad de Ciencias Exactas y Naturales, Universidad Nacional de Mar del Plata-CONICET Deán Funes 3350, B7602AYL Mar del Plata, Argentina*

[2]*Instituto de Investigaciones en Ciencia y Tecnología de Materiales (INTEMA), Universidad Nacional de Mar del Plata-CONICET Juan B. Justo 4302, B7608FDQ Mar del Plata, Argentina*

(Received 7 March 2012; published 11 June 2012)

The necklace model, which mimics the reptation of a chain of N beads in a square lattice, is used to study the drift velocity of charged linear polymers in gels under an applied electric field that periodically changes its direction. The characteristics of the model allow us to determine the effects of the alternating electric field on the chains' dynamics. We explain why chains of different N can be made to move in opposite directions with a nonuniform electric field with certain values of intensity and frequency. The key point is that, when alternating electric fields are applied, longer chains spend more time out of the steady-state regime than lower chains. Numerical results are obtained by means of Monte Carlo simulations and they are qualitatively in agreement with experiments of DNA migration in gel electrophoresis.

DOI: 10.1103/PhysRevE.85.061801 PACS number(s): 83.10.Kn, 05.40.−a

I. INTRODUCTION

Separation of DNA by size is a subject of great importance in biophysics due to its wide applications in genetics. In this area, the gel electrophoresis is one of the most studied techniques. At present, the basic physics mechanisms involved are not completely understood. Even today, with the help of numerical models, the problem remains controversial.

It is well known that the drift velocity of charged linear polymers in a gel, under a constant electric field, is independent of size for large chains making impossible their separation. However, for nonuniform electric fields, longer chains can be separated. Also, chains of different sizes can be made to move in opposite directions.

The pulsed-field electrophoresis technique, which exploits the relation between mobility and orientation of the chains in an external pulsed field, was independently proposed by Schwartz and Cantor and by Carle and Olson [1]. After that, different ways of applying variable electric fields in gel electrophoresis of linear chains have been proposed [2–6]. An excellent review was written by Viovy a few years ago [7].

The key step to the theoretical understanding of the dynamics of entangled polymer melts was made by de Gennes [8]. Afterwards, Doi and Edwards promoted the same idea [9]. de Gennes proposed that reptation is the main mechanism in the dynamics of polymers in a medium with a high density of obstacles, such as a gel or an entangled polymer melt. According to this idea, the chain cannot move sideways due to the surrounding obstacles that confine its motion to a one-dimensional diffusion along a tube. Therefore, the chain progresses by leaving part of the initial tube and creating a new part as it moves. Rubinstein introduced the first discrete model to study the dynamic of linear polymers in a medium with dense obstacles [10]. Later, Duke adapted the Rubinstein model to study gel electrophoresis of DNA [11].

In this work, we study the drift of linear chains in a gel under the presence of a changing external force. With the help of the necklace model [12–14], we obtain numerical results for an external force that changes its strength and direction periodically. From these results, we explain in detail why in experiments [6] the drift velocity of very large chains depends on size whereas this does not occur under a constant electric field.

II. THE MODEL

The linear chain, consisting of N beads, is represented by a string of particles and holes and is placed in a square lattice of constant a. The gel fibers (or other polymers), which play the role of obstacles, are represented by crosses [see Fig. 1(a)]. The distance between two consecutive particles of the chain can be a or, in the case that there is a hole between the particles, $2^{1/2}a$ or $2a$. No more than one site can be empty between two consecutive beads. A given lattice site can be occupied by more than a particle or a hole only when the chain crosses itself. The chain has two end particles and N–2 inner particles. Each end particle only has one pre-end particle, that is, the consecutive particle of this end particle along the chain. The number of holes can vary from 0 to N–1.

At each Monte Carlo step, one of the N particles of the chain is randomly chosen in order to jump and the time t is increased by $1/N$ so that, at a time interval equal to 1, every particle has, on average, one chance to be selected.

When external forces are not applied, the jumping rules of the model are as follows [see Fig. 1(b) with $\delta = 0$]:

(i) If the particle is located at the end of the chain and its nearest site is occupied by its corresponding pre-end particle, the end particle jumps with a probability per unit time $p_a/3$, to each of the three nearest sites that are not occupied by the pre-end particle [see Figs. 1(b) or 1(c) with $\delta = 0$]. Then, the total jumping probability per unit time is p_a. If the jump takes place, a hole is created.

*cmaldao@fi.mdp.edu.ar

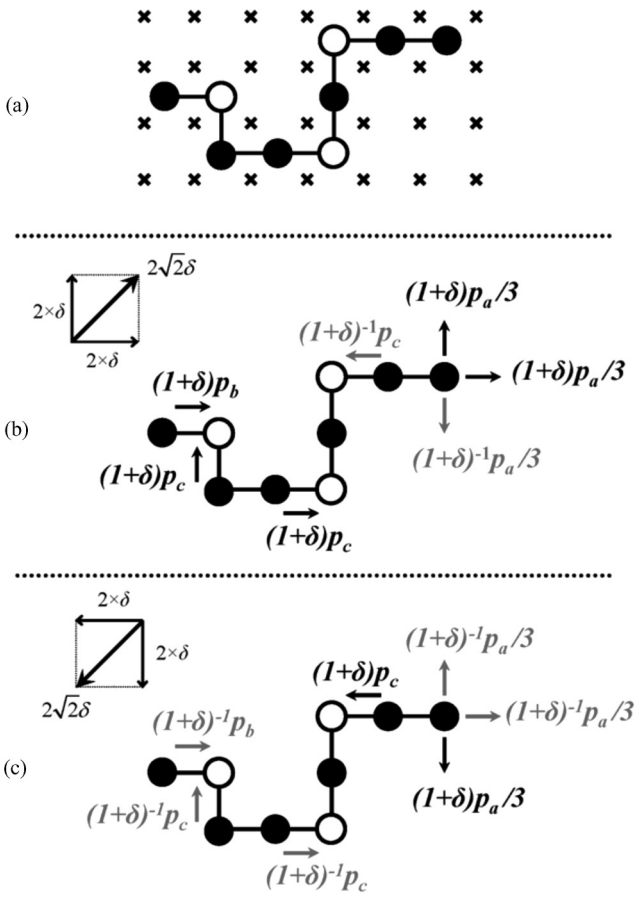

FIG. 1. Schematic representation of the two-dimensional necklace model. (a) Chains in a melt of other polymer chains or in a gel. Filled circles represent particles of the chain, open circles represent holes, and crosses represent the gel or other polymers that act as obstacles. (b) Jumping rates for end and middle particles when a forward external force is applied ($\delta > 0$). (c) Jumping rates for end and middle particles when a backward force is applied. In (b) and (c) the jumping rates for particles that can jump in the direction of the force are shown with black arrows; gray arrows correspond to jumps in the opposite direction. Moreover, the applied force to every particle is shown for each case.

(ii) If the particle is located at the end of the chain and its nearest site is empty (i.e., there is a hole between this particle and its pre-end particle), the end particle jumps to the hole with a probability per unit time p_b. If the jump takes place, a hole is annihilated.

(iii) If the particle is not an end particle (i.e., it is a middle particle) and one of its nearest sites along the chain is occupied and the other one is empty, the middle particle jumps towards the hole with a probability per unit time p_c.

(iv) A middle particle with both nearest sites along the chain, occupied or empty, cannot jump and remains at its original position [see the only particle without arrows in Figs. 1(b) and 1(c)].

Hence, p_a, p_b, and p_c are the free parameters in the necklace model ($0 \leqslant p_a, p_b, p_c \leqslant 1$). In the following, without loss of generality, we will adopt that the distance a between adjacent sites of the square lattice and the unit time are equal to 1. In this work, the Monte Carlo results were obtained using $p_a = p_b = 0.25$ and $p_c = 0.5$. With these values of the parameters, the hole distribution is uniform along the chain and, for $N \gg 1$, the chain length l is proportional to N (see Ref. [13]).

If there is an applied external field, implying a force to the right, the jumping rates of a particle to the right and to the left will be considered to be $(1+\delta)k$ and $k/(1+\delta)$, respectively. If the external field is reversed, the jumping rates of a particle to the right will be $k/(1+\delta)$ and to the left $(1+\delta)k$. k is the jumping frequency when no force is applied, $k = p_a/3, k = p_b$, or $k = p_c$, and $\delta \geqslant 0$. In what follows, in a general sense, we will refer to δ as the applied force to a particle of the chain. However, the external force applied to a particle has a net horizontal component of magnitude 2δ and another vertical component of the same magnitude. Thus, the net force applied to every particle is $2 \times 2^{1/2}\delta$; see Fig. 1(b) and 1(c).

We can also refer to the external force in terms of a dimensionless applied electric field E. Indeed, $1+\delta = \exp(E_x/2) = \exp(E_y/2)$, where $E_x = E_y = E/(2^{1/2}) = q_e E'_x a/k_B T = q_e E'_y a/k_B T$, where E'_x and E'_y are the actual electric field in the x direction and y direction, respectively. q_e is the electric charge of every particle and k_B is the Boltzmann constant. Note that for $\delta \ll 1$, $\delta \approx E$.

In the following sections we report results for small forces, i.e., $\delta \ll 1$. Mainly, we focus our study on the effects that a nonuniform external field produces on the drift velocity of the center of mass of the chains when $\delta \ll 1$ and $N \gg 1$. As is demonstrated in [15], under these conditions, the drift velocity is independent of N for a constant field.

III. RESULTS AND DISCUSSIONS

In this section we present and analyze in detail the effects of alternate electric fields on the drift velocity of the chains. During a time interval t_1, a forward force δ_1 is applied; next, a backward force δ_2 is applied in the opposite direction during the other time interval t_2. Figure 2 shows the external force as a function of time. Thus, the external force has a period $T = t_1 + t_2$. The values of the forces used in our Monte Carlo simulations were $\delta_1 = 0.005$ and $\delta_2 = -0.01$. The parameter q is defined as the ratio between t_1 and t_2, i.e., $q = t_1/t_2$.

We observed different behaviors for the mobility of the chains that depends on the way that the external force is

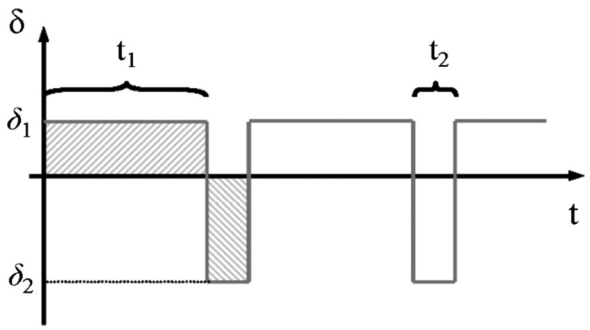

FIG. 2. Scheme representing the external force δ versus time t. In this work $\delta_1 = 0.005$ and $\delta_2 = -0.01$. t_1 represents the time interval in which the force acts "forward" and t_2 the time interval in which force acts "backward." The period of the force, T, is $T = t_1 + t_2$ and the parameter q is $q = t_1/t_2$.

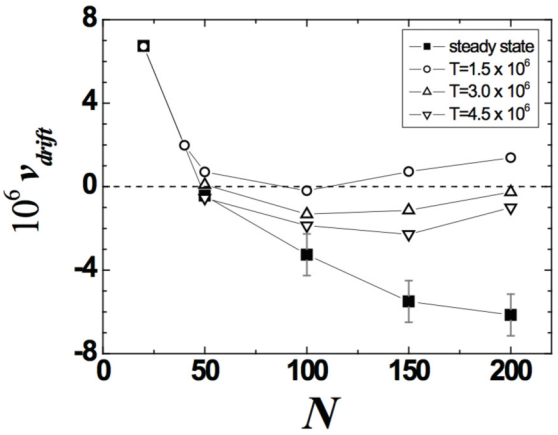

FIG. 3. Drift velocity of the center of mass of chains consisting of N beads for different periods of the external force. These data and their error bars were calculated from the values of Table I. The full square symbols can be seen as the limit $T \to \infty$. These results were obtained using $q = t_1/t_2 = 7/3$ and the same behavior was observed for other values of q. Monte Carlo results for cases $T = 1.5 \times 10^6$, $T = 3.0 \times 10^6$, and $T = 4.5 \times 10^6$ were obtained averaging over 500 samples. The error bars for each point cannot be seen in the graph because they are of a size similar to the symbols.

applied. For certain values of q and T, some chains can move in one direction and other chains in the opposite direction. Even if the average value of the external force is null [i.e., $\langle\delta\rangle = (t_1\delta_1 + t_2\delta_2)/(t_1 + t_2) = 0$], the drift velocity can be different from zero. With the values of forces used in this work (δ_1 and δ_2), when $q > 2$, $\langle\delta\rangle$ is positive (forward direction).

In previous works (see Ref. [16]), chains are assumed to travel with the steady-state velocity. However, as we will show below, chains in the necklace model do not travel with this velocity immediately after changing the direction of the external force.

Figure 3 shows numerical results for the drift velocity of the center of mass of chains when forces of different periods, but the same value of q ($q = 7/3 > 2$), are applied. These numerical results and the mean velocities that the chains would have if they moved with the steady-state velocities (forward during a time t_1 and backward during a time t_2) are shown. The steady-state velocity is defined as the drift velocity when the external force is constant. These values are shown in Table I;

TABLE I. Drift velocities of the center of mass of chains for the case in which the external force is constant. They are the same velocity values given in Fig. 2 of Ref. [15]. The steady-state drift velocities were calculated using these values (square full symbols of Fig. 3). Note that, considering the error bars, velocities for chains with $N \geqslant 150$ do not dependon N.

Drift velocities under constant electric field		
N	$10^5 v_{\delta=0.005}$	$10^5 v_{\delta=0.01}$
50	2.89 ± 0.1	6.90 ± 0.1
100	1.80 ± 0.1	5.30 ± 0.1
150	1.40 ± 0.1	5.10 ± 0.1
200	1.35 ± 0.1	5.20 ± 0.1
400	1.34 ± 0.1	5.20 ± 0.1

they correspond to the data of Fig. 2 in Ref. [15]. When external forces are not applied, these velocities are null.

The aim of using nonuniform electric fields in gel electrophoresis is to separate chains that cannot be separated with a uniform electric field. Within the model, for the used parameters, this occurs for chains with $N \geqslant 150$ (Table I). From Fig. 3, it is clear that, with increasing period, the drift velocity tends to the value of the velocity that the chains would have if they moved with the steady-state velocity (full square symbols). These results reveal that the mean velocity, due to the non-steady-state movement of the chains, decreases gradually with increasing the period of external force. This can be understood as follows. Let us call τ the time interval that a chain of N beads needs to reach the steady-state velocity after changing the direction of the external field. If the period T is small, let us suppose $T \approx \tau$, the chain does not move with the steady-state velocity because steady state is not reached. Conversely, for a large enough period T, $T \gg \tau$, the time interval τ for which the chain does not move with the steady-state velocity becomes negligible in comparison to the time the chain moves with the steady-state velocity. For this reason, with increasing T ($T \to \infty$), the mean velocity of the center of mass of the chains tends to the curve of square symbols in Fig. 3. Note that for a value of $T \approx \tau$ corresponding to a large chain, smaller chains can move most of the time with the steady-state velocity because the interval time τ decreases with the chains' size.

Using the steady-state velocities, the mean velocity (full square symbols in Fig. 3) for $N \geqslant 50$ is negative even when the mean force $\langle\delta\rangle$ is positive ($q > 2$). The reason is the following. For a given value of N, the steady-state velocity for a constant force has a nonlinear dependence with the external field δ. For example, for $N \geqslant 150$ (see Table I) the behavior of v is close to δ^2. In general, $v \sim \delta/N$ for $N\delta \ll 1$ and $v \sim \delta^2$ for $\delta \ll 1$ and $N \gg 1$ (see, for example, [15] and reference cited therein).

It is interesting to note in Fig. 3 that there are chains that move in the same direction of the average external force while other chains move in the opposite direction. Furthermore, some chains have an average velocity equal to zero (i.e., the center of mass of these chains oscillates around a fixed point). The value of N for having a null average velocity depends on T and q.

At this point, one wants to know how the chains react to the variable external force that makes them move so differently. To explain this interesting behavior, in Fig. 4 we compare the Monte Carlo numerical results for the displacement x, the velocity of the center of mass v, and the end-to-end distance of the chains r, versus time for $N = 150$ (left) and $N = 200$ (right). Parameters were chosen so that chains move in opposite directions. The direction of the external field is schemed at the top of the graphs and the gaps between dashed vertical gray lines correspond to each period of the field.

Results of Fig. 4 correspond to the steady-state chains' displacements under the applied alternate field. Specifically, chains were moved during a time of 50×10^6 before making measurements to guarantee that steady state was established. We checked that this was the case by assessing the chains and their movements. After that, chains were allowed to move for another 10 periods of 1.5×10^6, the interval in which the

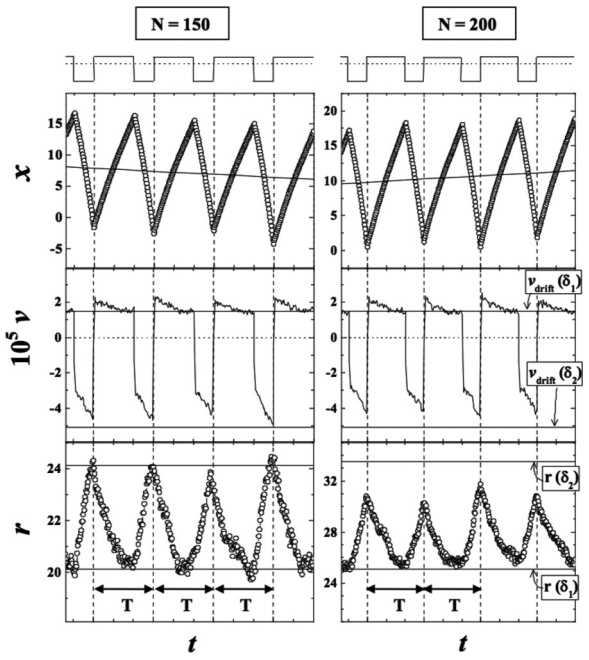

FIG. 4. Displacement x, velocity of the center of mass of the chains v, and end-to-end distance r versus time for chains with $N = 150$ (left) and $N = 200$ (right). Results were obtained using $T = 1.5 \times 10^6$ and $q = 2.125$. In the top, the time dependence of the external force is schemed. The gaps between dashed vertical lines correspond to periods of external force. In both upper graphs, the average displacements of the center of mass of the chains are indicated with straight lines. The slopes of these straight lines represent the average drift velocity of the chains along ten periods, $\langle v_N \rangle$ [$\langle v_{N=150} \rangle = (-4.0 \pm 0.4) \times 10^{-7}$ and $\langle v_{N=200} \rangle = (3.0 \pm 0.4) \times 10^{-7}$]. In both middle graphs, the instant velocity was calculated from the derivatives of the upper graphs. The values of the velocities that the chains would have if they moved with the steady-state velocity are indicated with horizontal lines [$v(\delta_1)$ and $v(\delta_2)$]. In both lower graphs, the values of the end-to-end distances of the chains, for the case of uniform external force, are indicated with horizontal straight lines [$r(\delta_1)$ and $r(\delta_2)$].

average drift velocity was determined with the slope of the center of mass displacement.

In both upper graphs of Fig. 4, displacements of the center of mass of the chains are shown. With straight lines, the mean displacements of the center of mass of the chains are indicated. Note that, on average, for $N = 200$ the chains move forward and for $N = 150$ they move backward. In both middle graphs, which show the instant drift velocities, the values of the velocities that the chains would have if they moved with the steady-state velocity are indicated with horizontal straight lines [$v(\delta_1)$ and $v(\delta_2)$]. In both lower graphs, the values of the end-to-end distance of the chains are plotted; horizontal straight lines correspond to results for the case of uniform external force [$r(\delta_1)$ and $r(\delta_2)$].

Note that the second graph of Fig. 4 is the instant velocity of the center of mass of the chains determined as the derivative of the displacements shown in the first graph. Instant velocities to the right and to the left are on the order of 10^{-5}. The average velocity of the center of mass is a consequence of the difference between the displacements during the chain movement to the right and to the left. For the values of the parameters adopted, the average velocity is on the order of 10^{-7}, positive for $N = 200$ and negative for $N = 150$.

During the time interval t_1, in which the force δ_1 is applied to the right, the end-to-end distance diminishes until reaching the steady-state value (lower horizontal straight line). After the time interval t_1, the direction of the external force is changed to the left for a time interval t_2. Consequently, the end-to-end distance increases until reaching its corresponding steady-state value or until the direction of the external force is switched again to the right. It is important to note at this point that the stronger the external force, the larger the chains' stretching [15].

From graphs of instant velocity (middle graphs of Fig. 4), it stands out that chains need a time of about τ to reach the steady-state velocity after reversing the direction of the external field. Sometimes chains never reach the steady-state velocity (observed in Fig. 4 when the field is backward). However, an appreciable difference between velocities for $N = 150$ and $N = 200$, which explains why chains of different size can move in opposite directions, is not easily detected.

In the lower graphs of Fig. 4, which represent the end-to-end distance of the chains, one can appreciate a significant difference between numerical results for $N = 150$ and $N = 200$. Similarly to the results for instant velocities, after switching the direction of the external field, the chains need a time τ' to reach the end-to-end distance corresponding to steady state.

Note that τ and τ' have different magnitudes; τ corresponds to the velocity and τ' to the end-to-end distance of the chains. For chains of $N = 150$, when the external force is applied during a time t_2 to the left, the chains reach the steady-state value of the end-to-end distance approximately when the external force changes again. From this, we can say that $\tau'_{N=150} \approx t_2$. As expected, for longer chains ($N = 200$) the time required to stretch them to the steady-state value is greater because of the larger number of particles that form the chains (i.e., $\tau'_{N=200} > \tau'_{N=150}$). As it occurs in the absence of obstacles, longer chains are also easier to stretch when obstacles are present. This can be observed in Fig. 3 of Ref. [15]; for longer chains under a given small external field, the stretching per bead increases with N. Thus, beads of longer chains have to overcome a larger number of obstacles after applying or changing the external field before chains reach the steady-state configuration. For this reason, chains of $N = 200$ cannot stretch completely when the force is applied backward during a time t_2. In other words, when the direction of the external force is switched, longer chains are further away from the steady-state configuration. This means that larger chains remain more coiled than shorter chains, which directly affects their movement. It has been shown that the drift velocity is favored in stretched chains [15]; hence, chains of $N = 150$ move faster than chains of $N = 200$ during t_2. It is interesting to note that stretching mainly takes place along the direction of the applied field, with the stretching in the perpendicular direction being only a few percent of that in the direction of the field.

In brief, the basic mechanism responsible for the observed results is the following. During the time interval t_2, when the external force is applied backward, chains of $N = 200$ are not in

steady state for a longer time (more coiled) than shorter chains. Accordingly, the difference between the backward velocity and the steady-state velocity is greater for chains with $N = 200$ than for chains with $N = 150$. Thus, longer chains present a net forward drift velocity. Now, we can understand the results shown in Fig. 3, where $q = 2.33$ (in Fig. 4, $q = 2.125$). For example, results corresponding to $T = 1.5 \times 10^6$ indicate that the end-to-end distances of the chains reach the corresponding steady-state value for $N < 50$. For this reason the velocity decreases with N (longer chains have lower velocity). Instead, for $N \geqslant 100$, longer chains do not reach the steady state when the force is backward. Thus, long chains can have velocities that, on average, are positive.

The numerical results shown here explain why chains of different sizes can move in opposite directions. If our goal is to separate those chains, we must know the dispersion of the center of mass as a function of time, $\sigma(t)$, compared to the distance between mean positions of the center of mass of the chains. We observed that the dispersion grows as the square root of time (i.e., $\sigma \approx t^{1/2}$). Conversely, the distance between the center of mass of the chains increases linearly with time. Therefore, chains of different sizes can be separated as dispersions grow slower with time than the distance between mean positions.

IV. CONCLUSIONS

In recent years, the applications of various fields have been very useful in extending the size limit of DNA molecules in gels that can be separated. In many works, the drift velocity in the presence of a force that changes its direction has been studied. However, the effects that this kind of external force causes in the dynamics of linear chains are not well explained.

In this paper, as a natural extension of our previous work with the repton model, we studied in detail the effects of a variable force on chains with different sizes. We saw that chains, which cannot be separated by size with a uniform force, can be separated for certain values of intensity and frequency of an external field. To explain this result, which is experimentally observed [6], we proposed a straightforward argument developed by analyzing the dynamics of the chains when the direction of external force is reversed. We observed that, after inverting the direction of the external field, the chains do not move with the steady-state drift velocity. This is the "key" to explaining the separation of chains with nonuniform external fields.

In summary, it is well known that experimentally long chains cannot be separated with uniform external fields but they can be separated with alternating electric fields. As shown in this paper a possible mechanism, which emerges naturally in the necklace model, arises as a result of the chains moving out of steady state.

ACKNOWLEDGMENTS

This work was partially supported by the National Council for Scientific and Technical Research (CONICET) of Argentina (PIP 0041/2010-2012), and the National University of Mar del Plata (Argentina).

[1] D. C. Schwartz and C. R. Cantor, Cell **37**, 67 (1984); G. F. Carle and M. V. Olson, Nucleic Acids Res. **12**, 5647 (1984).
[2] G. F. Carle, M. F. Frank, and M. V. Olson, Science **232**, 65 (1986).
[3] T. A. J. Duke and J. L. Viovy, Phys. Rev. Lett. **68**, 542 (1992).
[4] H. Tsai, T. Y. Low, S. Freeby, A. Paulus, K. Ramnarayanan, C. P. Cheng, and H. E. Leung, Proteome Sci. **5**, 18 (2007).
[5] J. Kauttonen, J. Merikoski, and O. Pulkkinen, Phys. Rev. E **77**, 061131 (2008).
[6] L. L. Frumin, S. E. Peltek, S. Bukshpan, V. V. Chasovskikh, and G. V. Zilberstein, Phys. Chem. Comm. **3**, 61 (2000); L. L. Frumin, S. E. Peltek, and G. V. Zilberstein, Phys. Rev. E **64**, 021902 (2001).
[7] J. L. Viovy, Rev. Mod. Phys. **72**, 813 (2000).
[8] P. G. de Gennes, J. Chem. Phys. **55**, 572 (1971); P. G. de Gennes, *Scaling Concepts in Polymer Physics* (Cornell University Press, Ithaca, NY, 1979).
[9] M. Doi and S. F. Edwards, *The Theory of Polymers Dynamics* (Clarendon Press, Oxford, 1986).
[10] M. Rubinstein, Phys. Rev. Lett. **59**, 1946 (1987).
[11] T. A. J. Duke, Phys. Rev. Lett. **62**, 2877 (1989).
[12] S. E. Guidoni, H. O. Mártin, and C. M. Aldao, Eur. Phys. J. E **7**, 291 (2002); Phys. Rev. E **67**, 031804 (2003).
[13] G. R. Terranova, C. M. Aldao, and H. O. Mártin, Phys. Rev. E **76**, 031111 (2007).
[14] A. Buhot, Eur. Phys. J. E **18**, 239 (2005).
[15] G. R. Terranova, H. O. Mártin, and C. M. Aldao, Physica A **388**, 2149 (2009).
[16] G. W. Slater, S. Guillouzic, M. G. Gauthier, J. F. Mercier, M. Kenward, L. C. McCormick, and F. Tessier, Electrophoresis **23**, 3791 (2002).